Atmospheric Environment 244 (2021) 117973

Contents lists available at ScienceDirect

Atmospheric Environment

journal homepage: http://www.elsevier.com/locate/atmosenv

Comparison of reactive gaseous mercury measured by KCl-coated denuders and cation exchange membranes during the Pacific GEOTRACES GP15 expedition

Yipeng He, Robert P. Mason *

Department of Marine Sciences, University of Connecticut, 1080 Shennecossett Road, Groton, CT 06340, USA

HIGHLIGHTS

- Hg speciation in the MBL over the Pacific was quantified during 2018 GEOTRACES GP15.
- A comparison measurement of RGHg by a KCl-coated denuder and CEM showed differences.
- RGHg measured by CEM was on average 5 times higher than the value from the denuder.
- This study suggested RGHg was underestimated using the KCl-coated denuder over MBL.
- High RGHg was found with low ozone and there was a diurnal cycle in the tropics.

ARTICLE INFO

Keywords:
Mercury
Reactive gaseous mercury
KCl-Coated denuder
Cation exchange membrane
Pacific
GEOTRACES GP15

ABSTRACT

Reactive gaseous mercury (RGHg) over the marine boundary layer (MBL) has been investigated in many oceans, such as the North Atlantic, Arctic and Antarctic using the KCl-coated denuder, as deployed in the Tekran instrument. Given recent concerns on the suitability of the denuder for capturing RGHg, we initiated a comparison study of RGHg concentrations measured by the KCl-coated denuder and with cation exchange membranes (CEM) during the Pacific GEOTRACES GP15 cruise between Alaska and Tahiti along 152°W from 18 September to November 24, 2018. RGHg concentrations measured by the KCl-coated denuder showed a strong variability along the cruise and ranged from 0.2 to 42.2 pg/m^3 (average 7.2 pg/m^3), while RGHg collected by the CEM similarly showed a large variability with a range from 10.7 to 143.3 pg/m^3. However, a different pattern spatially and temporally was seen with the two measurement devices. Overall, RGHg concentrations measured by the CEM were, on average, 5 times higher than those measured by the KCl-coated denuder. In addition, the Tekran data suggest that occasional daily peaks of RGHg were associated with ozone depletion providing evidence for the formation of RGHg by reactions with reactive halogen species. A diurnal cycle in the RGHg concentration was observed in the low latitude tropical regions, likely caused by these photochemical reactions. Although the measurements by the denuder have better time resolution, and allow for examination of processes for RGHg formation, their efficiency of capture of RGHg needs to be further considered. This study suggested that using the KCl-coated denuder led to an underestimation of RGHg over the MBL, as found in previous studies. Therefore, further studies should be made to examine the measured RGHg concentrations over the MBL using different quantification approaches to further examine the distribution of RGHg.

1. Introduction

Due to rapidly increased human activity, such as coal combustion, gold mining and industrial production, the amount of mercury (Hg) released to the biosphere has been substantially enhanced since antiquity (Driscoll et al., 2013; Engstrom et al., 2014; Lamborg et al., 2014). In the atmosphere, three major species of inorganic Hg are defined by their chemical and physical properties as elemental Hg (Hg^0), reactive gaseous Hg (RGHg) and particulate Hg (Hg^P), with some fractions being operationally defined (Landis et al., 2002; Laurier et al.,

* Corresponding author.
E-mail address: robert.mason@uconn.edu (R.P. Mason).

https://doi.org/10.1016/j.atmosenv.2020.117973
Received 26 May 2020; Received in revised form 16 September 2020; Accepted 25 September 2020
Available online 3 October 2020

2003; Sheu and Mason, 2001). Mercury speciation fluctuates dramatically in the environment as the dominant species vary with medium and location, and this results in a diverse fate for atmospheric deposition within the global Hg cycle. Usually, Hg^0, as the main species in the atmosphere (~97% of the total atmospheric Hg), has a long atmospheric lifetime with the range of six months to one year (Holmes et al., 2006). The resultant long-range atmospheric transport of emitted Hg^0 from natural and anthropogenic sources, contrasts with that of RGHg and Hg^P, which have relatively short lifetimes of about 1–10 h in the near-surface atmosphere, due to their reactivity, and they are readily deposited by wet or dry deposition mechanisms (Holmes et al., 2009). Generally, RGHg is less than 10 pg/m^3 and comprises just around 1% of atmospheric Hg in the lower troposphere (Lindberg et al., 2007). However, due to its high reactivity with water, it can deposit within a 100 km radius of its production location, and become a major contributor to Hg in wet deposition, even given its low concentration (Holmes et al., 2009). So, the local formation of RGHg could become a critical local Hg component of air-sea exchange and should be considered in any calculations. Several cruises have investigated the composition of atmospheric gaseous Hg across the oceans by using the Tekran speciation system, as it simultaneously can determine the three species of inorganic Hg (Landis et al., 2002). Laurier et al. (2003) showed RGHg concentrations varied from 0.15 to 92.4 pg/m^3 with an average of 9.5 pg/m^3 in the North Pacific and the negative relationship with ozone strongly suggested the *in-situ* formation of RGHg by photochemical reaction with halogens which was also observed in the year-round measurements in the MBL over the Galápagos Islands in the equatorial Pacific (Wang et al., 2014). Aspmo et al. (2006) showed that RGHg concentrations ranged from 0 to 22 pg/m^3 with an average of 2.4 pg/m^3 in the North Atlantic. Temme et al. (2003) reported RGHg concentrations over the South Atlantic with a range of 1–30 pg/m^3 with the mean concentration as 8 pg/m^3. Also, Soerensen et al. (2010) suggested a global mean of RGHg in the free marine boundary layer (MBL) was 3.1 ± 11 pg/m^3, based on the data from prior studies.

At present, a controversy has re-emerged regarding the precision of measuring RGHg by using the Tekran speciation system, which measures RGHg based on trapping it with a potassium chloride (KCl)-coated denuder as the first separation step (Landis et al., 2002). The trapping efficiency of the denuder for all components that make up RGHg has been questioned and oppugned (Huang et al., 2013; Jaffe et al., 2014) and concerns raised that environmental variables (i.e., ozone and humidity) could also impact the suitability of measuring RGHg by a KCl-coated denuder (Huang and Gustin, 2015). Concerns over the efficiency of the denuders for trapping RGHg were also raised in earlier studies (Sheu and Mason, 2001). Some evidence suggests that absolute humidity and ozone have an inverse correlation with RGHg recovery by the denuder, examined using a known source of RGHg (i.e., $HgBr_2$). These studies inferred that the KCl-coated denuder method could underestimate RGHg concentrations in the atmosphere (Huang and Gustin, 2015; McClure et al., 2014). An alternative method has been proposed to capture RGHg by using in-line filters with cation exchange membranes (CEM), which have been used already to determine RGHg concentrations in ambient air in previous studies (Ebinghaus et al., 1999; Huang et al., 2013, 2017; Mason et al., 1997b; Sheu and Mason, 2001). In one international field inter-comparison at Mace Head, Ireland, RGHg collected by a series of two CEMs with an up-front quartz fiber filter was determined to range from 13 to 23 pg/m^3 while RGHg collected by the KCl-coated denuder showed a higher concentration range from 41 to 94 pg/m^3, but it was thought that this was due to potential aerosol influence (Ebinghaus et al., 1999). Another field campaign in the Chesapeake Bay area measuring the speciation of atmospheric Hg, compared using a five-stage Teflon filter pack (one quartz fiber filter and four CEMs in sequence), a denuder and refluxing mist chambers, suggested that the denuder could be underestimating the RGHg concentration, although the differences were not always consistent (Mason et al., 1997a; Sheu and Mason, 2001). In addition, Huang et al. (2013) suggested that the CEM, and additionally a nylon filter, measured 1.3 to 3.7 times higher RGHg than the KCl-coated denuder in both laboratory and field experiments, further demonstrating the underestimation of RGHg concentrations by the denuder. However, despite these field and lab experiments on the comparison, the potential limitations and concerns associated with the CEM have not been conclusively demonstrated for active sampling. Several studies have mentioned the concern of the re-oxidization of Hg^P captured on the upstream particulate filters then being captured on the downstream CEM as RGHg and alternatively, possible adsorption of RGHg to the particulate filters (Gustin et al., 2015; Miller et al., 2019). In addition, the CEM could have an artifact as, under high relative humidity, the condensation of water vapor on the CEM surface, could absorb ozone from the atmosphere during the sampling period, which would cause additional RGHg formation on the CEM from the passing Hg^0. Such reactions could also occur on an upstream particulate filter. These limitations and concerns were still unsolved prior to the cruise.

Given the recent concern about the efficiency of the KCl-coated denuder and the previous experiments using alternative methods, in this study we examined the speciation of atmospheric Hg over the marine boundary layer where few comparisons have been made with multiple approaches. For measuring RGHg, the Tekran speciation system and the multistage filter pack were used during the GEOTRACES Cruise to help us better understand the RGHg concentrations in the MBL. This paper focuses on the comparison of measuring RGHg between these two approaches and compares the results with data from other studies.

2. Materials and methods

2.1. Cruise information

The U.S. GEOTRACES GP15 cruise (Pacific Meridional Transect), which is a section of the U.S. GEOTRACES program, was conducted in the central Pacific Ocean along 152°W from 56°N to 20°S between Alaska and Tahiti (Fig. 1a). The R/V *Roger Revelle* (Fig. 1c; https://scripps.ucsd.edu/ships/revelle) departed from Washington (Seattle) on September 18, 2018 and sailed northwest up to the Alaska shelf and then headed south, with a two-day stop at Hawaii (Hilo) from 21 to 24 October, until reaching Tahiti (Papeete) on November 24, 2018. The cruise supported a large amount of individual scientific projects studying the biogeochemical interactions of trace elements and isotopes (TEIs), not only in the ocean, but also in the near-surface atmosphere (https://www.geotraces.org/gp15-geotraces-cruise).

2.2. RGHg measurement by the KCl-coated denuder

2.2.1. Sampling on ship

Measurements of Hg speciation in the near-surface atmosphere were made by using the Tekran speciation system (2537B/1130/1135; Tekran Inc.) for determination of Hg^0, RGHg and Hg^P, respectively, which was also used on the 2015 U.S. Arctic GEOTRACES cruise (DiMento et al., 2019) and the 2002 Intergovernmental Oceanographic Commission (IOC) cruise transect over the North Pacific Ocean (Laurier et al., 2003). The Tekran speciation system was deployed on the front rail of the 03 deck of the ship at a height of approximately 10 m above sea level to minimize the influence from the stack (Fig. 1b; Fig. 2; Supporting Information S1). After the initial instrument external calibration using the Tekran 2505 calibration unit while in the port, manual injections were repeated to check the calibration on the Tekran 2537B biweekly and the recovery was between 95% and 107%, with the average of 98%. In addition, the internal permeation source calibrations of Tekran 2537B were performed every 25 h, so it was calibrated at different times every day. The detection limits for the Tekran speciation system were estimated at < 0.1 ng/m^3, 1.0 pg/m^3 and 1.0 pg/m^3 for Hg^0, RGHg and Hg^P, respectively (Landis et al., 2002; Tekran, 2005). The Tekran speciation system was typically set up for a sampling time of 1 h for all species and a

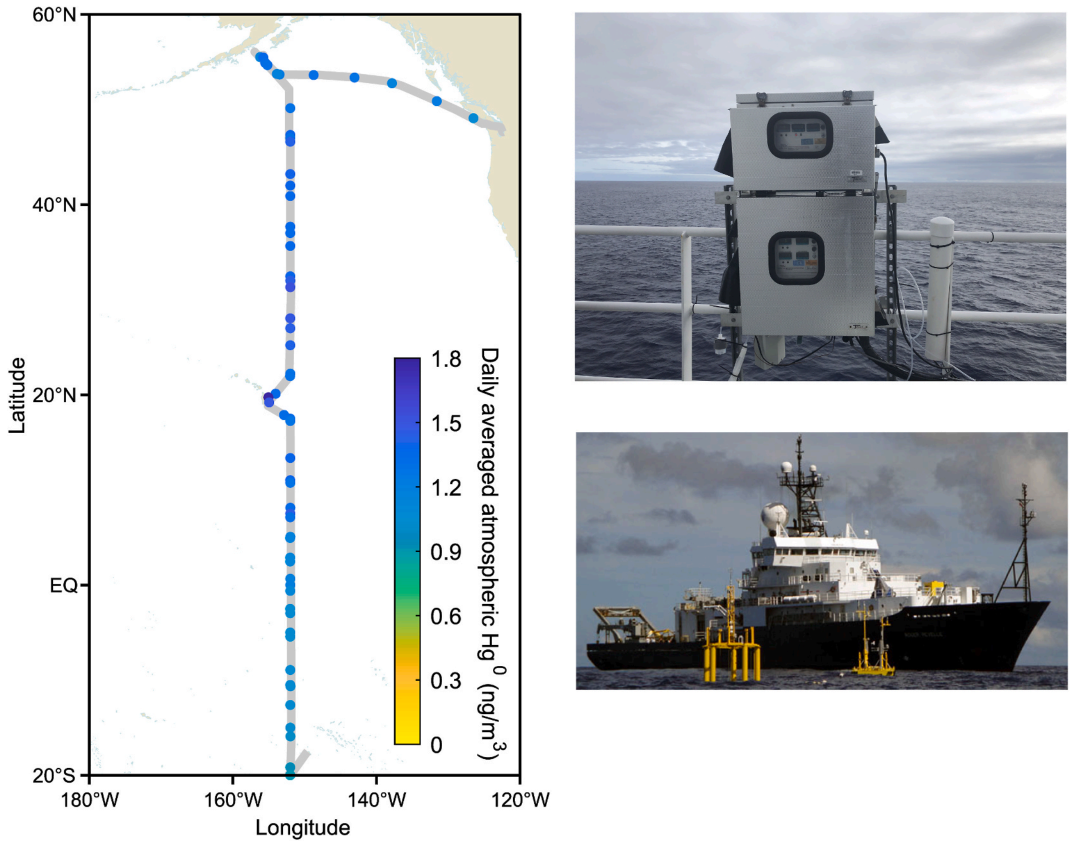

Fig. 1. The U.S. Pacific GEOTRACES GP15 cruise and Tekran speciation system on the front rail of R/V Roger Revelle. (a) The U.S. GEOTRACES GP15 cruise track shown as the grey line in the central Pacific Ocean along 152°W from 56°N to 20°S between Alaska and Tahiti, 18 September - November 24, 2018. The colored dots along the cruise track represent the daily averaged atmospheric Hg^0 measured by Tekran 2537B; (b) the Tekran speciation system mounted on the front rail of the 03 deck of the ship at a height of approximately 10 m above sea level; and (c) The R/V Roger Revelle (https://scripps.ucsd.edu/ships/revelle).

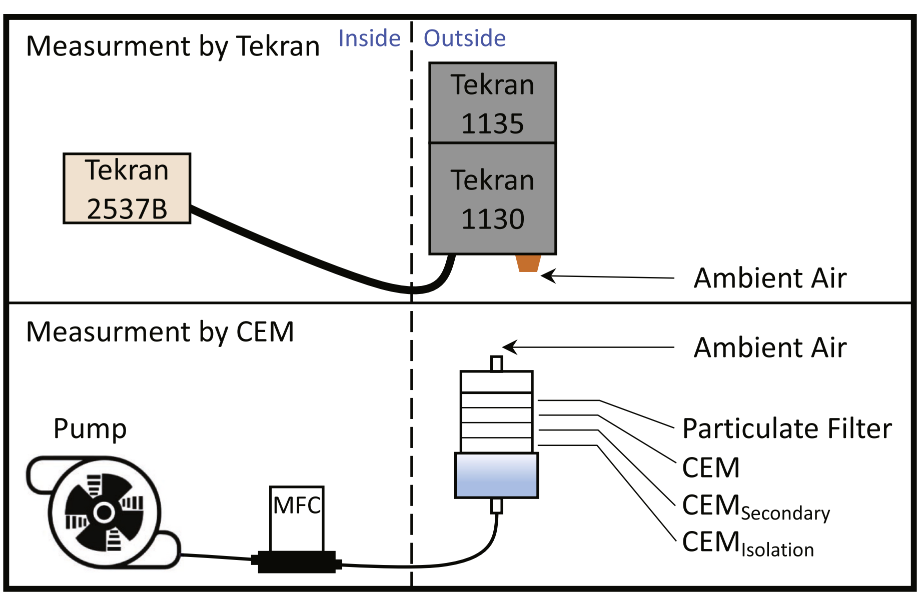

Fig. 2. Schematic diagram of the apparatus for measuring atmospheric mercury speciation by the Tekran speciation system, and particulate and reactive gaseous mercury (RGHg) by the Teflon multistage filter pack. In the top panel, ambient air intake through the Tekran 1130/1135 mounted outside on the front rail of the 03 deck of the ship and passed through the 10 m heating line to the Tekran 2537B inside the ship's lab. In the bottom panel, the Teflon multistage filter pack mounted outside with four filters. Ambient air drawn through the filter pack using a diaphragm pump with a mass flow controller to determine air flow.

desorption time of 1 h for RGHg and Hg^P, so a full cycle of sample duration was 2 h. By pumping the ambient air through the inlet with a heated impactor (removal of the coarse particle fraction > 2.5 μm), RGHg and Hg^P were then absorbed firstly onto the KCl-coated denuder and then on the particulate trap of the Tekran 1130/1135, respectively, while Hg^0 was quantified with a Tekran 2537B, with a 5 min time resolution. After a 1 h sampling period, the pyrolyzer, particulate trap and denuder were heated to 800 °C, 800 °C and 500 °C, respectively, while pumping zero-air into the system. Subsequently, RGHg and Hg^P were thermally desorbed and decomposed and transported into zero air and analyzed as Hg^0 by the Tekran 2537B.

2.2.2. Data analysis of atmospheric RGHg

Prior to analyzing the data generated from Tekran speciation system, a data validation process has been applied to remove the data corresponding to the following conditions: 1) the ship was stopped at the vertical profile stations during the transect, 2) the wind direction was relative to the ship's bow within $\pm 30^{\circ}$. These conditions stated above could allow compounds from ship's chimney into the inlet of Tekran speciation system, leading to the samples being contaminated. At each step within the cycle of the Tekran speciation system sample duration, an event flag number was associated with each step as 0, 1, 2 and 3 for sample duration, zero air flush, particulate trap heat and denuder heat, respectively. The regular calculation of RGHg concentrations for each 15 min heating cycle was derived by summing up the three concentrations for the 5 min timesteps and subtracting three times the averaged blank concentrations, calculated from averaging the five concentrations during the system blanking period (flag number as 1), then multiplying by the conversion factor. Usually, the five concentrations with the flag number as 1 (blanks) were similar to each other, from 0.1 to 0.5 ng/m^3. However, during the cruise, some cycles showed two higher flush blank concentrations, with one at the beginning of the zero-air flush into the system and the other one following the denuder heating step (Supporting Information S2; Fig. S1), which also happened before the cruise when we tested the Tekran speciation system at University of Connecticut, Avery Point campus. If we included these two higher flush blank concentrations, which likely reflected Hg^0 released from the speciation units, in the regular calculation of RGHg concentrations, it would likely overestimate the blank concentrations and underestimate the RGHg concentrations. To address this issue, an adjustment was applied in the regular calculation by ignoring the first blank concentration and treating the second blank concentration as additional RGHg from the denuder heating. Additional analytical details are included in the Supporting Information S2.

2.3. RGHg measurement by the CEM

2.3.1. Sampling on ship

According to our experience from previous studies (Mason et al., 1997b; Sheu and Mason, 2001), the multistage Teflon filter pack was deployed and mounted close to the inlet of Tekran speciation system to make the datasets comparable to each other (Fig. 2). The multistage Teflon filter holder included four filters in order from the air intake: one quartz fiber filter (0.2 μm pore size, 47 mm dia.) to remove particles and three polyethersulfone acidic negatively charged cation exchange membranes (CEM; I.C.E. 450, 0.45 μm pore size, 47 mm dia., Pall Corp.) – as the capture RGHg filter, a backup filter to assess for "breakthrough" of RGHg from the previous filter, and a filter to stop any back contamination from the pump and Teflon tubing when the pump is switched on/off during sampling. Ambient air was drawn through the filter pack using a diaphragm pump with a mass flow controller (MFC; GFC3, Aalborg Inc.) to determine the air flow. The Teflon tubing (about 10 m) ran from the front rail of the 03 deck and down a gooseneck conduit into the ship's interior connected to the pump. The air flow rates were around 2 L/min and each filter pack was deployed for a total sampling period of 2–3 days to obtain a detectable signal above the detection limit (DL) of 90 pg, which is equivalent to 10 pg/m^3 RGHg given the typical volumes collected. Deployment details for each filter pack, and more QA/QC information are included in the Supporting Information S1 (Table S1). Filter packs were acid cleaned in a procedure described by Landis and Keeler (1997) and double-bagged for storage and transfer, and sample filters were stored frozen in polystyrene petri dishes (Fisherbrand, Fisher Scientific Co.) and acid digested prior to analysis for Hg, as detailed below. Filters were loaded into and unloaded from the filter pack in a High Efficiency Particulate Air (HEPA) filter blower within a plastic bubble clean space constructed in the laboratory of the ship to avoid any potential contamination from the lab air. In addition, the pump was controlled by an automated sector-control system to prevent contamination from the ships' emissions, with the cycling between on and off being determined by the wind speed/direction relative to the ship speed/direction. Therefore, the pump was activated at periods when the relative wind direction was from within $\pm 60^{\circ}$ of the ship's bow and a relative wind speed was above 0.5 m/s, for at least five continuous minutes to avoid the ship's stack exhaust (Marsay et al., 2018). In addition, deployment blanks of the filter pack were collected during the cruise by loading but not deploying the filter packs and they were stored in the same manner as sample filters. As noted above, the CEM filters were used and compared to the Tekran speciation system prior to the cruise at the University of Connecticut, Avery Point campus to ascertain the differences between the two collection methods for marine air, and the results are detailed in the SI.

2.3.2. Analysis of the CEM

All filters were stored frozen in polystyrene petri dishes which were double-bagged and shipped to University of Connecticut, Avery Point campus for the analysis of total Hg concentrations. Details of the analytical method is provided in the Supporting Information S3 and is summarized here. Each CEM was transferred to an individual 15 ml polypropylene centrifuge tube (Fisherbrand, Fisher Scientific Co.) and digested with 4.5 M nitric acid (HNO_3; TraceMetal Grade, Fisher Chemical, Fisher Scientific Co.) in a covered water bath (Precision Model 184, GCA Corp.) at about 60 °C for 12 h. The digested solution was further oxidized with bromine monochloride (BrCl) to convert all Hg species to divalent Hg (Hg^{II}) and subsequently pre-reduced with hydroxylamine hydrochloride ($NH_2OH{\bullet}HCl$) to consume the excess BrCl. The solution was then further reduced with stannous chloride ($SnCl_2$) to convert all Hg^{II} to Hg^0, which was quantified by dual gold-amalgamation with cold vapor atomic fluorescence detection (CVAFS) using an automated Tekran 2600 system, in accordance with U.S. EPA Method 1631 Revision E (Bloom and Fitzgerald, 1988; DiMento et al., 2019; Fitzgerald and Gill, 1979; U.S. Environmental Protection Agency, 2002). The system background Hg was checked for each analytical run by analyzing the solution with only pure reagents in the same vials for each batch of 5 filters sample, analyzed in triplicate. The precision and recovery were determined by analyzing total Hg standards before and after each batch, and the mean recovery for all Hg standards was 101.2 ± 7.1%, and the detection limit (DL) was 0.25 pM.

Also, as done in other studies, so-called filter breakthrough was calculated for each filter pack by comparing total Hg concentrations on the first and secondary CEM using Eq. (1).

$$Breakthrough(\%) = \frac{CEM_{2nd} - CEM_{Blank}}{(CEM_{1st} - CEM_{Blank}) + (CEM_{2nd} - CEM_{Blank})} \times 100 \tag{1}$$

While high concentrations on the backup (second) filter has been attributed to the lack of capture of RGHg on the first CEM filter, we discuss other explanations for the presence of RGHg on the second filter. CEM blanks were collected, stored and analyzed in the same manner with every set of sample filters, and each CEM sample subtracted the corresponding CEM blank to calculate the final blank corrected concentration for data analysis.

2.4. Ozone and auxiliary data for the atmosphere

In order to understand the extent of halogen chemistry and ozone depletion in the MBL (Holmes et al., 2009), ozone was quantified using an UV photometric ozone analyzer (Model 49i, Thermo Fisher Scientific Inc.), which was calibrated prior to the cruise at port and during the cruise on a weekly basis. Unfortunately, the analyzer had analytical issues after the ship stopped at Hawaii (Hilo), therefore, ozone data for Leg 2 is not available. In addition, the Shipboard Meteorological Acquisition System (MetAcq) measured and recorded a wide variety of meteorological data: air temperature, barometric pressure, wind speed/direction, relative humidity, photosynthetically active radiation

(PAR), seawater temperature and seawater conductivity (Fig. S4). Atmospheric meteorological sensors were generally located on the forward part of the ship or above the ship's upper bridge deck. Details about the sensor types could be found at the R/V *Roger Revelle* main website (https://scripps.ucsd.edu/ships/revelle).

3. Results and discussion

3.1. Spatial and temporal variation of RGHg in the Pacific

3.1.1. Tekran speciation system results

According to the meridional transect, trends of RGHg concentration in the Pacific Ocean can be divided into five zones based on geographical and hydrographical settings (Soerensen et al., 2014) – the coastal region (47°N - 56°N - 50°N), the North Pacific (50°N - 13°N), the intertropical convergence zone (ITCZ; 13°N - 5°N), the equatorial zone (5°N - 1°S) and the South Pacific (1°S - 20°S). Generally, RGHg concentrations varied spatially and temporally throughout the cruise, as shown in Fig. 3, from the coastal region to the open ocean. In this study, RGHg data showed a strong variability along the cruise track, and ranged from 0.2 to 42.2 pg/m^3, with averaged value of 7.2 pg/m^3. Overall, the data suggested the *in-situ* production of RGHg by photochemical processes with reactive halogen species.

Within the coastal region zone, during the first two weeks of the transect, when the ship was near to the coast of Alaska, RGHg concentrations measured by the Tekran speciation system were 8.8 ± 2.8 pg/m^3, with a small and stable variation compared to the results from the other zones. In agreement, Laurier et al. (2003) also reported that the RGHg concentrations near the coast of Japan during the 2002 IOC cruise ranged from 0.2 to 10.7 pg/m^3, which were comparable to the measurements in this study, while measurements made within the Arctic region showed a much lower mean of RGHg concentrations about 1.7 pg/m^3 (DiMento et al., 2019). In addition, there was a small diurnal cycle, characterized by increased midday maxima, near the coast of Alaska. The weather was windy and cold, and cloudy conditions prevailed. Ozone concentrations were variable, with a range from 2 to 20 ppbv.

At the end of the first two weeks, the ship encountered a significant storm, which eliminated the power supply for the Tekran speciation system, and therefore, no measurements by the Tekran were made during and after the storm for one week. However, the measurements by the CEM were continued during the storm. RGHg concentrations showed significantly lower values after the storm to the north of the North Pacific zone (Wilcoxon Rank Sum Test, p-value < 0.001), which suggested that the higher wet deposition during this time had removed the RGHg from the atmosphere. Also, in this zone, between 47°N and 34°N, RGHg concentrations were the lowest among the whole transect, with a mean value as 2.3 pg/m^3.

Between 34°N and 13°N, RGHg concentrations showed a higher variability, with a range in concentration from 0.5 to 32.6 pg/m^3 (average 9.1 pg/m^3). Also, some instances of increased RGHg were associated with apparent ozone depletion (Fig. S3), which suggested the *in-situ* formation of RGHg by halogen reactions (Holmes et al., 2009). However, the overall trend of ozone concentrations had no significant correlation with the RGHg concentrations, which suggests that other processes also influenced the RGHg, besides reactions that produced ozone depletion. Near the island of Hawaii, higher RGHg concentrations and variability were found, which were comparable to the measurements made around the Hawaiian Islands during the 2002 IOC cruise (Laurier et al., 2003). These data suggested potential RGHg sources from the islands.

Within the ITCZ, where a higher frequency of rain events happened, RGHg concentrations were low and varied from 2.8 to 15.5 pg/m^3, with an averaged value of 7 ± 2.6 pg/m^3. Therefore, we propose that RGHg was being actively removed from the atmosphere to the surface ocean by wet deposition, which supported an enhanced Hg pool at the ocean surface, and which could support the higher evasion of dissolved Hg^0 back to the atmosphere (Soerensen et al., 2014). In correspondence with

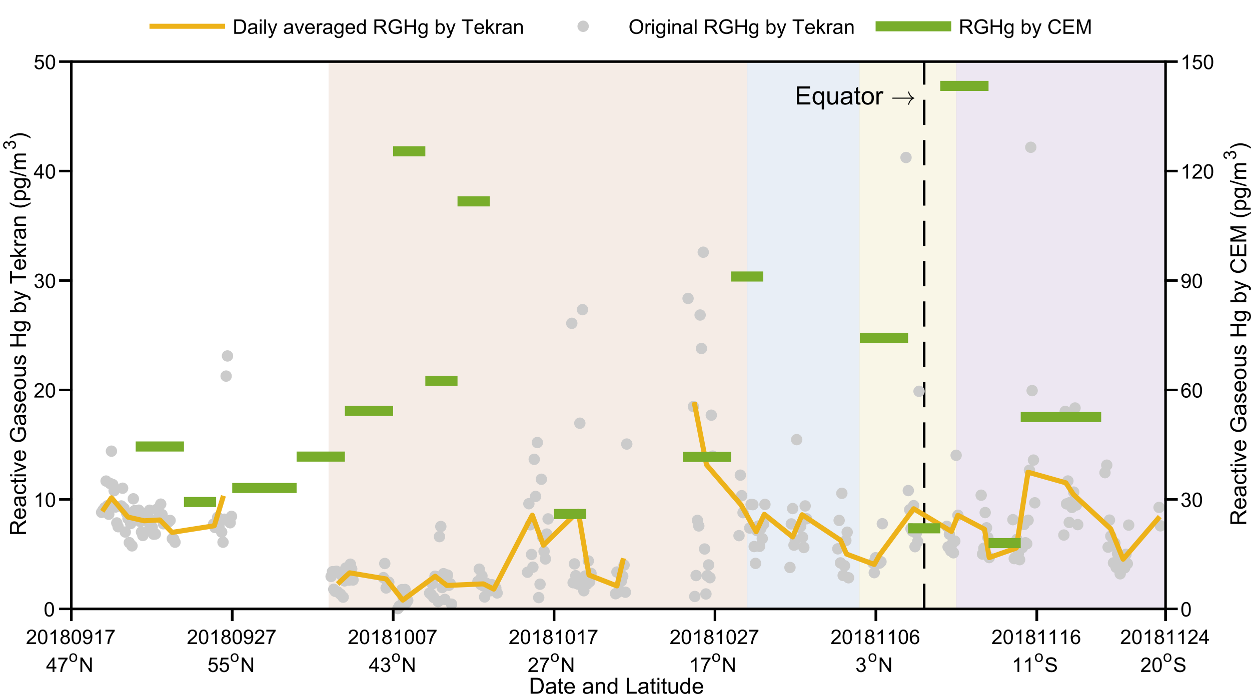

Fig. 3. Atmospheric RGHg concentrations measured by the Tekran (left axis scale) and the CEM (right axis scale) during the U.S. Pacific GEOTRACES GP15 cruise. Reactive gaseous mercury concentrations in atmosphere are plotted against the sample date and latitude. Original RGHg concentrations and daily averaged RGHg concentrations measured by the Tekran are shown in grey dots and the yellow line is the daily average, respectively. RGHg concentrations measured by the CEM are shown as a green horizontal bar representing the sample duration. The dashed line represents the equator. The different background colors represent the five zones along the cruise track, as described in the text. (For interpretation of the references to color in this figure legend, the reader is referred to the Web version of this article.)

a higher wet deposition for RGHg, an increased formation rate for RGHg would also be needed to sustain the RGHg concentration in the atmosphere. Unfortunately, ozone data was not available after the ship passed the Hawaiian Islands. A previous cruise, from 50°N to 15°S along 170°W, showed that ozone concentrations had a dramatic decrease at the ITCZ from around 20 ppb–2 ppb (Johnson et al., 1990), suggesting the influence of reactive halogen reactions on both ozone depletion and on RGHg production.

In the equator zone and the South Pacific zone, RGHg concentrations were 8.4 ± 8.1 pg/m^3 and 8.4 ± 5.8 pg/m^3, respectively, and showed no significant difference between each other (Wilcoxon Rank Sum Test, *p*-value = 0.35). For these low latitude regions, typical tropical areas, the measurements characterized that RGHg concentrations had a diurnal cycle corresponding to the photochemical reactions, as indicated by the solar radiation, with a RGHg peak at midday (Fig. S2), which was also observed by previous studies (Laurier and Mason, 2007; Laurier et al., 2003; Soerensen et al., 2010). A recent study reported year-round measurements of Hg^0 and RGHg along with ozone and halogen oxides in the MBL over the Galápagos Islands in the equatorial Pacific showed that higher level of RGHg occurred around the midday and suggested an additional oxidant was needed to reproduce the high midday RGHg concentrations, which was also generated by photochemistry (Wang et al., 2014).

3.1.2. CEM results

To better compare the CEM RGHg results with those from the Tekran speciation system, all RGHg concentrations were plotted together in Fig. 3, with a three times larger scale for the CEM data than the Tekran speciation system data. Generally, RGHg collected by the CEM showed a larger variability spatially and temporally with a range from 10.7 to 143.3 pg/m^3 but seemed to display a unique pattern compared to the Tekran results.

According to previous studies, several environment variables and the functioning of the CEM filters should be discussed before considering any further explanation of the RGHg pattern. Uptake of Hg^0 by the CEM during active sampling must be ruled out for successfully using them for ambient RGHg measurements, as even a small amount of Hg^0 uptake (1%–2%) would easily overwhelm the detection of ambient RGHg. However, Stratton et al. (2001) found when using the refluxing mist chamber to collect RGHg that the presence of a filter upstream of the device had no impact on the RGHg concentration. Some studies have also shown that Hg^0 uptake on CEM material was negligible, even under a high Hg^0 exposure ranging from 1.43×10^6 to 1.85×10^6 pg/m^3 (Miller et al., 2019), which means that during the lower Hg^0 exposure during the Pacific sampling (i.e. sampling in the open ocean), Hg^0 trapping was not an issue.

In addition, there was a constant high humidity condition on the ship during the sampling with the relative humidity values often over 80%. Previous studies have shown that the recovery of RGHg concentrations measured on the CEM positively correlated with the atmospheric relative humidity, up to 91% at high relative humidity (>45%) (Huang and Gustin, 2015). However, a shortcoming was also noted corresponding to the high relative humidity, which caused a higher RGHg collection on the CEM. This effect is thought to occur from the condensation of water vapor on the CEM surface, which could absorb ozone from the atmosphere during the sampling period, which could result in additional RGHg formation on the CEM by the passage of Hg^0 over them. This could lead to the potential overestimation of RGHg on the CEM. Also, water vapor could induce condensation even on the downstream filters, which also could have caused higher concentrations on this filter, and which could result in a high "breakthrough" on the second CEM in some instances. Thus, if such reactions did occur, then the high concentration on the second filter is not from breakthrough, but from chemical reactions occurring on the membrane. In this study, most of the breakthrough values were 0–30% of the values on the first CEM, with three extremes over 40%, which were much higher compared to previous studies (Huang et al., 2013; Miller et al., 2019). The results with the high relative values on the second filter are not plotted in Fig. 3, but the information is reported in Table S1.

The trend of RGHg concentrations measured by the CEM showed low values near the coast of Alaska, with a range from 29.2 to 33.5 pg/m^3, and higher values, with a range from 10.7 to 143.3 pg/m^3, toward the open ocean, showing a similar trend to the Tekran data. However, the RGHg concentrations measured by the CEM showed no rain removal effect after the storm, nor within the ITZC, compared to the Tekran measurements. We hypothesize that this is due to the possible *in-situ* formation of RGHg on the CEM during the sampling at high relative humidity/wet conditions. Comparing our data to the global mean RGHg concentration in the free MBL, estimated as 3.1 ± 11 pg/m^3 based on the data from previous studies (Soerensen et al., 2010), RGHg concentrations measured by the CEM in the Pacific were much higher and not in a comparable range. Other measurements made by the CEM in the Atlantic Ocean showed a high range of RGHg concentrations from 50 to 700 pg/m^3 (Mason et al., 2001), which suggested a higher estimation of RGHg in the MBL using the CEM.

3.2. Comparison of RGHg based on the two methods

For better comparison between the RGHg concentrations measured by the CEM and the Tekran, RGHg concentrations from the Tekran were averaged over the same period during the CEM sampling. In this study, RGHg concentrations measured by the CEM were constantly higher than those measured by the Tekran. At the lower RGHg range (<45 pg/m^3) measured by the CEM, RGHg concentrations were 1–4 times higher than those measured by the KCl-coated denuder, while a lower ratio was apparent with higher RGHg concentrations (>45 pg/m^3), as shown in Fig. 4, which indicates a lower collection efficiency for the KCl-coated denuder. Also, RGHg measurements from this study were comparable to previous studies that compared these sampling devices, with the same linear trend (Gustin et al., 2019; Huang et al., 2013; Luippold et al.,

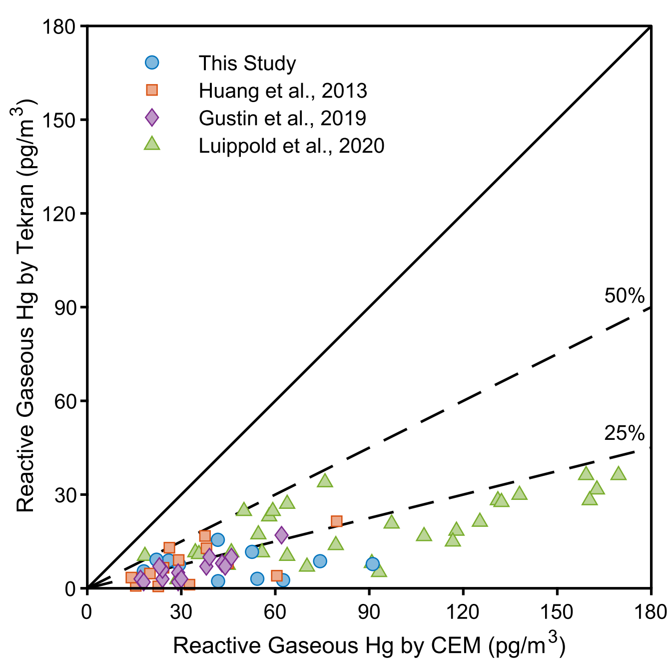

Fig. 4. Comparison of RGHg measured by the Tekran speciation system (left axis) with that measured by the CEM filters (bottom axis). Blue cycle, red square, purple diamond and green triangle denote the data from this study, Huang et al. (2013), Gustin et al. (2019) and Luippold et al. (2020), respectively. The solid line is the 1:1 comparison. Two dash lines represent the 50% and 25% comparison. (For interpretation of the references to color in this figure legend, the reader is referred to the Web version of this article.)

2020), for which the linear correlation, including all the previous data, was:

$$RGHg_{Denuder} = 0.17 \times RGHg_{CEM} + 2.0$$

with $r^2 = 0.62$ (p-value < 0.001). As the linear regression should pass through the origin, theoretically if the blanks are properly determined for each instrument, this relationship would be:

$$RGHg_{Denuder} = 0.19 \times RGHg_{CEM}$$

with $r^2 = 0.60$ (p-value < 0.001). The coefficients of this linear correlation indicated that the CEM measured 5 times higher RGHg than the KCl-coated denuder in these field experiments, on average, which concurs with the other studies that also inferred the underestimation of RGHg concentrations by the denuder.

It should be stated that the differences between the two devices cannot be accounted for by the potential artifact of RGHg collection by the CEM from high humidity conditions during the cruise. As noted above, these so-called breakthrough values were mostly <30% of that on the primary CEM filter. Even if we assume that all this RGHg is due to formation on the moist filter surface due to ozone reactions, this is a small difference that cannot account for the much larger differences in the values recorded by the CEM and the Tekran denuder. However, it is clear that further testing is needed to get a better estimation of the potential for this artifact to influence measurements with the CEM.

3.3. Comparison of RGHg based on adjusted Tekran data

As stated in Section 2.2.2, a high flush blank was observed after the denuder heat step in a full cycle on some occasions, which indicated the potential underestimation of calculated RGHg by the regular calculation process. An adjusted calculation process, taking into account the potential for low reporting of RGHg by the denuder, has been applied and compared to the regular calculation process, as detailed in the Methods. There was some improvement in the comparison, as shown in Fig. 5. By characterizing the improvement as the relative change in the ratios between RGHg concentrations measured by KCl-coated denuder and CEM, the overall improvement was 80 ± 106%, which indicated the regular calculation process may miss quantifying RGHg to a substantial degree on some occassions. Within the low RGHg range (<45 pg/m^3), as indicated by the CEM measurements, the adjusted process showed an increased estimated capture of RGHg of about 90 ± 120%, while at the high RGHg range (>45 pg/m^3), the adjusted process only increased the estimated capture of RGHg by about 50 ± 14%. Although the adjusted calculation process improved the results from the Tekran, the capture efficiency, assuming the CEM capture was 100%, was still not comparable to the CEM measurements.

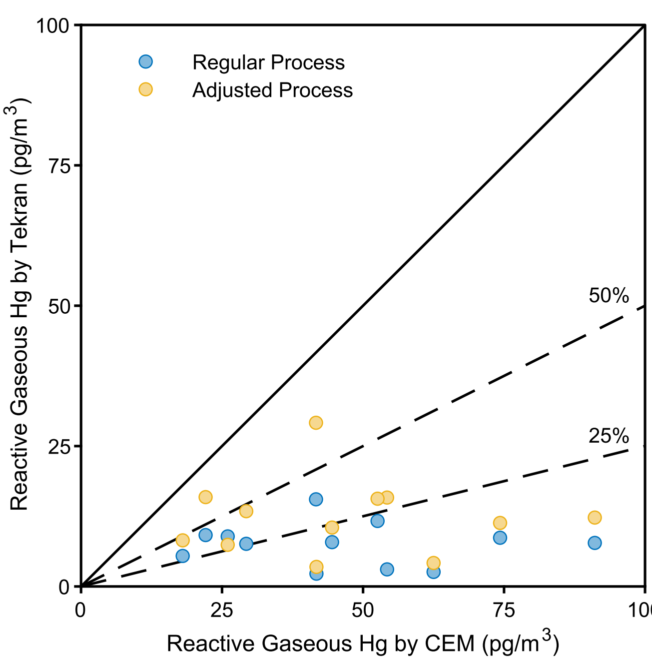

Fig. 5. Comparison of RGHg measured by Tekran speciation system with and without the adjusted calculation process (left axis) with that measured by the CEM (bottom axis). Blue and yellow circles represent the data without and with the adjusted calculation process for RGHg concentration measured by the Tekran. The lines are as in Fig. 4. (For interpretation of the references to color in this figure legend, the reader is referred to the Web version of this article.)

Overall, while the CEM approach provides a higher estimate of the RGHg concentration in the boundary layer, the Tekran speciation system has the advantage of allowing the examination of changes on short time scales. On this cruise, the long collection time of the CEM cannot allow for any investigation of the diurnal variation in RGHg, and the causes for such changes, and does not allow for a detailed examination of the relationship between RGHg and other environmental variables. A much shorter sampling time for the CEM or another alternative approach is clearly a needed goal for their future use in environmental studies of RGHg concentrations and the controlling factors. Additionally, further studies are needed to examine both collection methods to further characterize potential artifacts with the methods, such as the potential for formation of RGHg on the CEM surfaces when sampling under conditions of high humidity.

4. Conclusion

Comparison of RGHg measurements collected using the KCl-coated denuder, as deployed in the Tekran instrument, and the CEM during a research expedition in the Pacific Ocean provided new evidence on the validity of previous estimations of RGHg concentrations within the MBL. RGHg data measured by the Tekran showed a strong variability along the cruise and ranged from 0.2 to 42.2 pg/m^3 (average 7.2 pg/m^3), which suggested that *in-situ* production of RGHg by photochemical processes with halogens was occurring in this region, as suggested by other field studies and modeling (Holmes et al., 2009; Laurier et al., 2003; Soerensen et al., 2010). The decrease of RGHg concentrations after the storm and during rain events indicated its high reactivity with water, and its importance as a contributor to Hg in wet deposition, as previously suggested (Laurier and Mason, 2007). By inspecting the ozone data along with the RGHg data, some increases of RGHg were associated with ozone depletion supporting the notion for the formation of RGHg by reactive halogen compounds. However, the overall trend of ozone concentrations had no significant correlation with the change of RGHg concentrations, which suggests other processes, such as mixing and deposition (wind speed), temperature, or heterogeneous reactions on surfaces, affect the RGHg concentration so that its concentration doesn't correspond closely with the ozone depletion, as noted by others (Laurier and Mason, 2007). For the low latitude regions, as typical tropical areas, the measurements were characterized by a diurnal cycle of RGHg, which was in correspondence with the photochemical reactions indicated by the solar radiation, with a RGHg peak at midday.

In comparison to the denuder collections, RGHg collected by the CEM showed a larger variability with a range from 10.7 to 143.3 pg/m^3. Overall, however, there was a different pattern spatially and temporally compared to the Tekran results. Due to the constant high humidity during the sampling, RGHg could have been produced at the CEM filter surface, which could have made the reported RGHg concentrations higher than the actual values. Also, a higher breakthrough was noted on the backup filter under these circumstances, suggesting the potential for Hg reactions on the filter surface.

This study showed that RGHg concentrations measured by the CEM were, on average, 5 times higher than those measured by the KCl-coated denuder, which suggested the underestimation of RGHg by the Tekran, as the potential artifact with the CEM under high humidity conditions cannot account for the large differences in values. By using the adjusted process for calculating the RGHg concentrations from the Tekran, the relative changes on the ratios between RGHg concentrations measured by KCl-coated denuder and CEM improved to 80% overall, but the improvements were not large enough to make the measurements comparable, and still suggests the insufficient trapping efficiency of the denuder. Therefore, this study inferred that an underestimation of RGHg over the MBL could happen in this region if the Tekran is used, and this should be considered when evaluating previous studies using the KCl-coated denuder. However, the longer sampling time of the CEM system did not allow these data to be used to examine the processes affecting RGHg concentration, which could be assessed with the Tekran data. Overall, more investigation of RGHg over the MBL should be made using various techniques and further studies are needed using the two approaches, and other techniques, in the future. Our understanding will be hampered until a reliable and robust technique is developed for the accurate and precise measurement of RGHg in the marine and terrestrial boundary layer.

Declaration of competing interest

The authors declare that they have no known competing financial interests or personal relationships that could have appeared to influence the work reported in this paper.

Acknowledgments

We would like to thank the captain and crew of the R/V *Roger Revelle*, as well as our colleagues on the U.S. GEOTRACES GP15 cruise, especially the atmospheric sampling group (Buck, Marsay and Landing). We also acknowledge the provision of a backup Tekran 2537A from Environment Canada, the Tekran 2505 calibration unit from Dr. Dan Jaffe's lab, and the HEPA filter blower unit from Dr. Carl Lamborg's lab. We would also like to thank Bridget Holohan, Dennis Arbige and Robert Dziomba for helping with pre-cruise preparation and shipping. This study was funded by the National Science Foundation (NSF) Chemical Oceanography Program grant number 1736659, and the results will be part of the thesis of Yipeng He.

Appendix A. Supplementary data

Supplementary data to this article can be found online at https://doi.org/10.1016/j.atmosenv.2020.117973.

References

Aspmo, K., Temme, C., Berg, T., Ferrari, C., Gauchard, P.-A., Fain, X., Wibetoe, G., 2006. Mercury in the atmosphere, snow and melt water ponds in the north Atlantic Ocean during Arctic summer. Environ. Sci. Technol. 40 (13), 4083–4089.

Bloom, N., Fitzgerald, W.F., 1988. Determination of volatile mercury species at the picogram level by low-temperature gas chromatography with cold-vapour atomic fluorescence detection. Anal. Chim. Acta 208, 151–161.

DiMento, B.P., Mason, R.P., Brooks, S., Moore, C., 2019. The impact of sea ice on the air-sea exchange of mercury in the Arctic Ocean. Deep Sea Res. Oceanogr. Res. Pap. 144, 28–38.

Driscoll, C.T., Mason, R.P., Chan, H.M., Jacob, D.J., Pirrone, N., 2013. Mercury as a global pollutant: sources, pathways, and effects. Environ. Sci. Technol. 47 (10), 4967–4983.

Ebinghaus, R., Jennings, S.G., Schroeder, W.H., Berg, T., Donaghy, T., Guentzel, J., Kenny, C., Kock, H.H., Kvietkus, K., Landing, W., Mühleck, T., Munthe, J., Prestbo, E. M., Schneeberger, D., Slemr, F., Sommar, J., Urba, A., Wallschläger, D., Xiao, Z., 1999. International field intercomparison measurements of atmospheric mercury species at Mace Head, Ireland. Atmos. Environ. 33 (18), 3063–3073.

Engstrom, D.R., Fitzgerald, W.F., Cooke, C.A., Lamborg, C.H., Drevnick, P.E., Swain, E.B., Balogh, S.J., Balcom, P.H., 2014. Atmospheric Hg emissions from preindustrial gold and silver extraction in the Americas: a reevaluation from lake-sediment archives. Environ. Sci. Technol. 48 (12), 6533–6543.

Fitzgerald, W.F., Gill, G.A., 1979. Subnanogram determination of mercury by two-stage gold amalgamation and gas phase detection applied to atmospheric analysis. Anal. Chem. 51 (11), 1714–1720.

Gustin, M.S., Amos, H.M., Huang, J., Miller, M.B., Heidecorn, K., 2015. Measuring and modeling mercury in the atmosphere: a critical review. Atmos. Chem. Phys. 15 (10), 5697–5713.

Gustin, M.S., Dunham-Cheatham, S.M., Zhang, L., 2019. Comparison of 4 methods for measurement of reactive, gaseous oxidized, and particulate bound mercury. Environ. Sci. Technol. 53 (24), 14489–14495.

Holmes, C.D., Jacob, D.J., Mason, R.P., Jaffe, D.A., 2009. Sources and deposition of reactive gaseous mercury in the marine atmosphere. Atmos. Environ. 43 (14), 2278–2285.

Holmes, C.D., Jacob, D.J., Yang, X., 2006. Global lifetime of elemental mercury against oxidation by atomic bromine in the free troposphere. Geophys. Res. Lett. 33 (20).

Huang, J., Gustin, M.S., 2015. Uncertainties of gaseous oxidized mercury measurements using KCl-coated denuders, cation-exchange membranes, and nylon membranes: humidity influences. Environ. Sci. Technol. 49 (10), 6102–6108.

Huang, J., Miller, M.B., Edgerton, E., Sexauer Gustin, M., 2017. Deciphering potential chemical compounds of gaseous oxidized mercury in Florida, USA. Atmos. Chem. Phys. 17 (3), 1689–1698.

Huang, J., Miller, M.B., Weiss-Penzias, P., Gustin, M.S., 2013. Comparison of gaseous oxidized Hg measured by KCl-coated denuders, and nylon and cation exchange membranes. Environ. Sci. Technol. 47 (13), 7307–7316.

Jaffe, D.A., Lyman, S., Amos, H.M., Gustin, M.S., Huang, J., Selin, N.E., Levin, L., ter Schure, A., Mason, R.P., Talbot, R., Rutter, A., Finley, B., Jaeglé, L., Shah, V., McClure, C., Ambrose, J., Gratz, L., Lindberg, S., Weiss-Penzias, P., Sheu, G.-R., Feddersen, D., Horvat, M., Dastoor, A., Hynes, A.J., Mao, H., Sonke, J.E., Slemr, F., Fisher, J.A., Ebinghaus, R., Zhang, Y., Edwards, G., 2014. Progress on understanding atmospheric mercury hampered by uncertain measurements. Environ. Sci. Technol. 48 (13), 7204–7206.

Johnson, J.E., Gammon, R.H., Larsen, J., Bates, T.S., Oltmans, S.J., Farmer, J.C., 1990. Ozone in the marine boundary layer over the Pacific and Indian Oceans: latitudinal gradients and diurnal cycles. J. Geophys. Res.: Atmosphere 95 (D8), 11847–11856.

Lamborg, C.H., Hammerschmidt, C.R., Bowman, K.L., Swarr, G.J., Munson, K.M., Ohnemus, D.C., Lam, P.J., Heimbürger, L.-E., Rijkenberg, M.J., Saito, M.A., 2014. A global ocean inventory of anthropogenic mercury based on water column measurements. Nature 512 (7512), 65–68.

Landis, M.S., Keeler, G.J., 1997. Critical evaluation of a modified automatic wet-only precipitation collector for mercury and trace element determinations. Environ. Sci. Technol. 31 (9), 2610–2615.

Landis, M.S., Stevens, R.K., Schaedlich, F., Prestbo, E.M., 2002. Development and characterization of an annular denuder methodology for the measurement of divalent inorganic reactive gaseous mercury in ambient air. Environ. Sci. Technol. 36 (13), 3000–3009.

Laurier, F., Mason, R., 2007. Mercury concentration and speciation in the coastal and open ocean boundary layer. J. Geophys. Res.: Atmosphere 112 (D6).

Laurier, F.J.G., Mason, R.P., Whalin, L., Kato, S., 2003. Reactive gaseous mercury formation in the North Pacific Ocean's marine boundary layer: a potential role of halogen chemistry. J. Geophys. Res.: Atmosphere 108 (D17).

Lindberg, S., Bullock, R., Ebinghaus, R., Engstrom, D., Feng, X., Fitzgerald, W., Pirrone, N., Prestbo, E., Seigneur, C., 2007. A synthesis of progress and uncertainties in attributing the sources of mercury in deposition. AMBIO A J. Hum. Environ. 36 (1), 19–33.

Luippold, A., Gustin, M.S., Dunham-Cheatham, S.M., Zhang, L., 2020. Improvement of quantification and identification of atmospheric reactive mercury. Atmos. Environ. 224.

Marsay, C.M., Kadko, D., Landing, W.M., Morton, P.L., Summers, B.A., Buck, C.S., 2018. Concentrations, provenance and flux of aerosol trace elements during US GEOTRACES Western Arctic cruise GN01. Chem. Geol. 502, 1–14.

Mason, R.P., Lawson, N.M., Sheu, G.R., 2001. Mercury in the Atlantic Ocean: factors controlling air–sea exchange of mercury and its distribution in the upper waters. Deep Sea Res. Part II Top. Stud. Oceanogr. 48 (13), 2829–2853.

Mason, R.P., Lawson, N.M., Sullivan, K.A., 1997a. Atmospheric deposition to the Chesapeake Bay watershed—regional and local sources. Atmos. Environ. 31 (21), 3531–3540.

Mason, R.P., Lawson, N.M., Sullivan, K.A., 1997b. The concentration, speciation and sources of mercury in Chesapeake Bay precipitation. Atmos. Environ. 31 (21), 3541–3550.

McClure, C.D., Jaffe, D.A., Edgerton, E.S., 2014. Evaluation of the KCl denuder method for gaseous oxidized mercury using HgBr2 at an in-service AMNet site. Environ. Sci. Technol. 48 (19), 11437–11444.

Miller, M.B., Dunham-Cheatham, S.M., Gustin, M.S., Edwards, G.C., 2019. Evaluation of cation exchange membrane performance under exposure to high Hg0 and HgBr2 concentrations. Atmos. Measur. Tech. 12 (2), 1207–1217.

Sheu, G.-R., Mason, R.P., 2001. An examination of methods for the measurements of reactive gaseous mercury in the atmosphere. Environ. Sci. Technol. 35 (6), 1209–1216.

Soerensen, A.L., Mason, R.P., Balcom, P.H., Jacob, D.J., Zhang, Y., Kuss, J., Sunderland, E.M., 2014. Elemental mercury concentrations and fluxes in the tropical atmosphere and ocean. Environ. Sci. Technol. 48 (19), 11312–11319.

Soerensen, A.L., Skov, H., Jacob, D.J., Soerensen, B.T., Johnson, M.S., 2010. Global concentrations of gaseous elemental mercury and reactive gaseous mercury in the marine boundary layer. Environ. Sci. Technol. 44 (19), 7425–7430.

Stratton, W.J., Lindberg, S.E., Perry, C.J., 2001. Atmospheric mercury Speciation: laboratory and field evaluation of a mist chamber method for measuring reactive gaseous mercury. Environ. Sci. Technol. 35 (1), 170–177.

Tekran, 2005. Tekran Model 2537a, Model 1130 Mercury Speciation Unit and Model 1135 Particulate Mercury Unit. User Manuals, Toronto, Canada, p. 1135.

Temme, C., Einax, J., Ebinghaus, R., Schroeder, W.H., 2003. Measure ments of atmospheric mercury species at a coastal site in the Antarctic and over the south Atlantic Ocean during polar summer. Environ. Sci. Technol. 27, 22.

U.S. Environmental Protection Agency, 2002. Method 1631, Revision E: Mercury in Water by Oxidation, Purge and Trap, and Cold Vapor Atomic Fluorescence Spectrometry. US EPA Office of Science and Technology, Washington, D.C.

Wang, F., Saiz-Lopez, A., Mahajan, A.S., Gómez Martín, J.C., Armstrong, D., Lemes, M., Hay, T., Prados-Roman, C., 2014. Enhanced production of oxidised mercury over the tropical Pacific Ocean: a key missing oxidation pathway. Atmos. Chem. Phys. 14 (3), 1323–1335.